

Energy Collection from Water Flow Based on Single-Electrode Triboelectric Nanogenerators

Shuangyin Chen¹, Chengwang Xiong¹, Jianhua Liu² and Minyi Xu²

Received: 09 March 2024 / Accepted: 13 May 2024

© Harbin Engineering University and Springer-Verlag GmbH Germany, part of Springer Nature 2025

Abstract

As intelligent sensors for marine applications rapidly advance, there is a growing emphasis on developing efficient, low-cost, and sustainable power sources to enhance their performance. With the continuous development of triboelectric nanogenerators (TENGs), known for their simple structure and versatile operational modes, these devices exhibit promising technological potential and have garnered extensive attention from a broad spectrum of researchers. The single-electrode mode of TENGs presents an effective means to harness eco-friendly energy sourced from flowing water. In this study, the factors affecting the output performance were investigated using different structures of single-electrode solid-liquid TENGs placed in a circulating water tank. In addition, the solid–liquid contact process was numerically simulated using the COMSOL Multiphysics software, and significant potential energy changes were obtained for the solid–liquid contact and liquid flow processes. Finally, the energy generated is collected and converted to power several light-emitting diodes, demonstrating that solid–liquid TENGs can generate effective electrical power in a flowing water environment. Through several experimental investigations, we finally determined that the flow rate of the liquid, the thickness of the friction electrode material, and the contact area have the most significant effect on the output efficiency of TENGs in the form of flowing water, which provides a guide for improving their performance in the future.

Keywords Triboelectric nanogenerator; Single electrode; Circulating water flow; Green energy harvesting; Solid–liquid contact

1 Introduction

With the increasing popularity of wearable devices and miniaturized sensors, solving the issue of self-powering has become urgent (Wang, 2013; Mondal et al., 2022; Wang et al., 2023b). In recent years, numerous studies have focused on addressing this issue (Wang et al., 2018; Xue et al., 2022; Gao et al., 2023). By employing different methods, such as biomimicry (Li et al., 2020; Zou et al., 2022) and tactile sensing (Jiang et al., 2022; Li et al.,

2023a; Feng et al., 2024), various energy-harvesting devices have been developed (Lin et al., 2019; Wu et al., 2023; Zhang et al., 2023; Mudgal et al., 2024; Wang et al., 2024), thereby achieving self-powering of miniaturized sensors. The goal is to achieve energy self-sufficiency without relying on external power sources or frequent recharging (Fan et al., 2012; Rayegani et al., 2023). In this context, triboelectric nanogenerators (TENGs) play a crucial role by providing a novel and promising approach for energy harvesting in these devices (Wang 2020). For the collection of energy in flowing media, some scholars have adopted the method of kinetic energy conversion, ultimately using TENGs to collect energy, and have achieved satisfactory outputs (Li et al., 2023b; Li et al., 2023c; Li et al., 2024). However, solid–liquid TENGs also have potential in the field of miniaturized sensors (Choi et al., 2015; Li et al., 2018; Wang et al., 2021). Currently, there is no satisfactory explanation for the stable output-influencing factors of solid–liquid TENGs in the form of flowing water. Therefore, we aim to further explore the main influencing factors through the construction of a flowing water environment, which is of great value for improving the performance of sensors working in marine environments (Tan et al., 2022; Ye et al., 2023).

The principle behind solid–liquid friction-based nano-

Article Highlights

- In order to collect green energy from moving water, a new type of friction nano power generation single electrode is used.
- The main factors affecting the energy harvesting efficiency were studied, and the service life of the device was investigated.
- The contact area of the friction electrode and the flow rate of water in the pipeline have a great influence on the efficiency of energy collection.

✉ Chengwang Xiong
chengwang.xiong@hrbeu.edu.cn

¹ College of Shipbuilding Engineering, Harbin Engineering University, Harbin 150001, China

² Marine Engineering College, Dalian Maritime University, Dalian 116026, China

generators lies in contact electrification, commonly referred to as triboelectric charging (Wang et al., 2017; Cheng et al., 2024; Zhao et al., 2024). This process involves the spontaneous generation of charges on two surfaces that separate after initial contact (Baytekin et al., 2011; Wang et al., 2013; Lin et al., 2020; Armiento et al., 2022). Contact electrification represents a charge transfer phenomenon dependent on friction between the contacting surfaces (Sun et al., 2021; Wang et al., 2023a). Solid–liquid TENGs leverage this characteristic by inducing friction through the contact of water and another frictional medium, resulting in a charge transfer process leading to potential variation (Chung et al., 2018; Hu et al., 2020). The frictional electrification at the solid–liquid interface differs mechanistically from solid–solid interfaces, endowing solid–liquid TENGs with unique advantages. The liquid medium not only enhances contact but also facilitates the transfer of friction-induced charges, ensuring a larger contact area and density (Wang 2013; Nguyen et al., 2023a). To some extent, this distinct characteristic guarantees higher efficiency and longevity (Munirathinam et al., 2022; Nguyen et al., 2023b; Vu et al., 2024). Consequently, the study of solid–liquid friction-based nanogenerators is highly worthwhile.

Because of the distinctive performance of solid–liquid friction-based nanogenerators, the concept has garnered significant attention, leading to extensive research efforts. Several types of solid–liquid nanogenerators with special structures and applications have been reported, including processes where water droplets come into contact with friction electrodes to enable solid–liquid friction-based nanogeneration (McCarty and Whitesides 2008; Liu et al., 2018; Nie et al., 2019; Nguyen and Ahn 2021; Li et al., 2022). However, the discontinuous availability of electrical output results from seasonal influences in this approach. Other studies exploited sudden changes in electrical signals induced by the solid–liquid contact process for ship liquid level sensors, efficiently detecting the draft of ships and marine platforms (Xu et al., 2019; Zhang et al., 2019). Some studies focused on the development of a single-electrode-mode TENG using polytetrafluoroethylene (PTFE)–copper (Cu) tubes and tap water, which harnesses the energy of flowing water. The collected electricity not only powers light-emitting diodes (LEDs) and scientific calculators but also provides continuous wireless monitoring for drop infusion systems and new insights into biomedical applications (Munirathinam et al., 2022). These studies collectively demonstrate a growing body of research on solid–liquid TENGs in recent years, specifically focused on energy-harvesting and self-powering sensors through water flow (Lee et al., 2019; Niu et al., 2020; Wang et al., 2020; Cui et al., 2022). Nonetheless, limited attention has been given to sustainable green energy collection from continuous water flow environments, and there is still a dearth of exploration into the primary factors affecting their output perfor-

mance. Thus, studying this aspect remains challenging.

In this work, we constructed a circulating water tank and used a variable-speed motor to adjust the flow rate of the water in the tank. We developed a novel single-electrode energy-harvesting device using PTFE tubes, Cu electrodes, and flowing water. The signal was collected using an electrostatic voltmeter, and the results were analyzed. Through multiple experiments, we investigated the effects of flow rate, contact area, diameter, material thickness, and other factors on the output performance. Because of the simple structure of WF-TENGs, this technology contributes to the development of single-electrode TENGs for energy harvesting from flowing water. This technology can also be used to harness energy from oceans, rivers, and other water bodies and applied to provide continuous energy for self-powered sensors.

2 Experimental

2.1 Setting up the experimental environment

To investigate the factors influencing the output performance of TENGs in the form of flowing water, we designed and constructed a circulating water tank with an adjustable flow rate for the water supply, as illustrated in Figures 1(a) and (b). The circulating water tank, shown in Figure 1(c), consists of six sections, namely, the power, experimental, diffusion, reflow, rectifier, and systolic sections. The dimensions of the tank are 1 480 mm in length, 400 mm in width, and 450 mm in height, and the tank is chiefly constructed from acrylic material. For sealing purposes, we used Kraft 705, a neutral and transparent silicone rubber adhesive known for its nontoxic and nonpolluting properties. Kraft 705 is suitable for a temperature range of -60°C to 100°C , ensuring stability and excellent sealing properties. The transparency of Kraft 705 enables the unobstructed observation of the contents of the tank during the experiments.

The power section, situated to drive the liquid flow within the flume, consists of essential components, such as a drive motor (41K25RA-C, 220 V; maximum speed of 1 350 r/min), coupling, paddle blade, shaft, and bearing. These components work in synergy to generate the necessary flow of liquid. The design sets the maximum flow rate of the liquid in the flume to be 3 m/s, which is reviewed as sufficient to meet the basic test conditions. To determine the signals, we directly connected an electrostatic meter (Keithley 6 514). Subsequently, signal acquisition was performed using the LabVIEW software, enabling real-time monitoring and data recording. This configuration enabled the real-time observation of signal variations throughout the experiments and the accurate documentation of collected data for subsequent analysis.

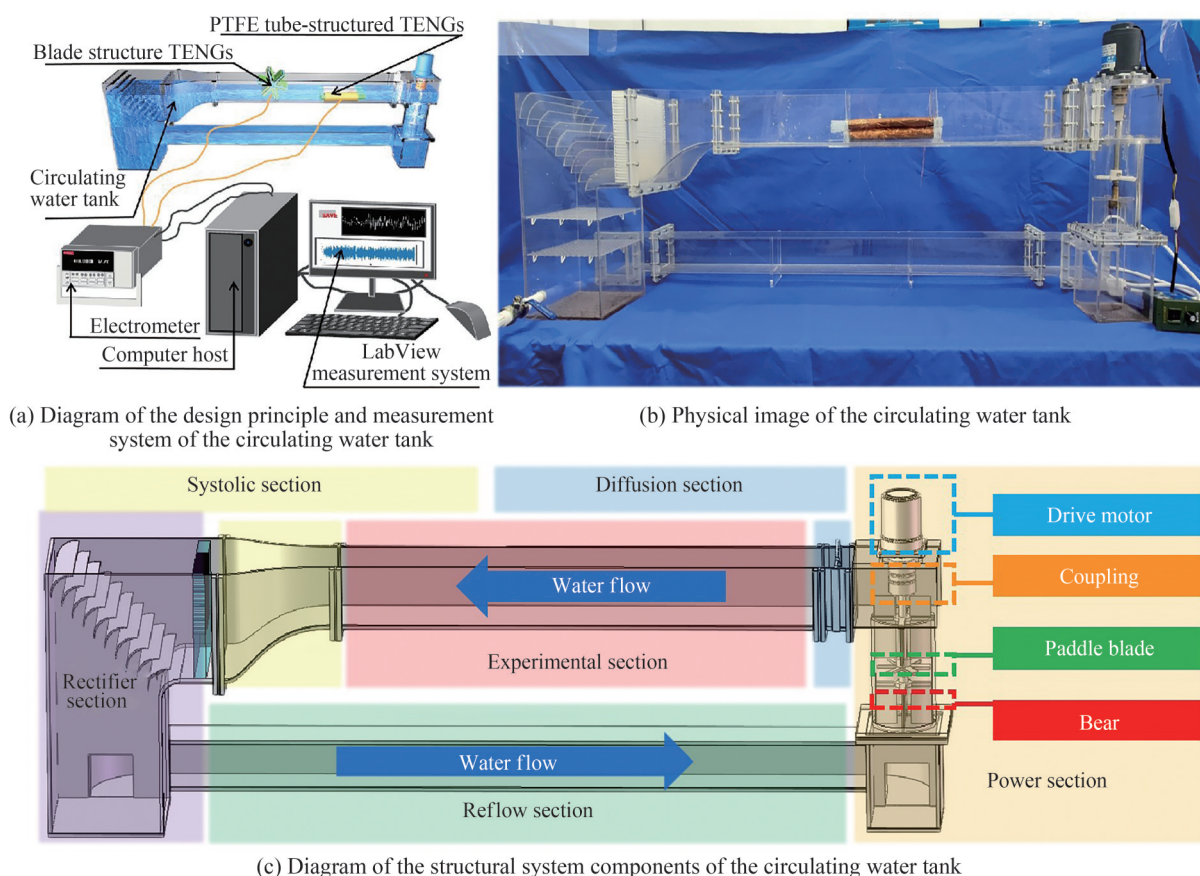


Figure 1 Experimental setup of the circulating water tank

2.2 Materials

In this experiment, the friction electrode is shaped like a single electrode and takes advantage of PTFE to form friction contact with the flowing water. The generated charge is transported via a 0.5 mm Cu ribbon, which has two-sided conductivity and is in close contact with the PTFE friction layer. Two principal forms of PTFE material, namely, a 0.1 mm thick PTFE film and a PTFE tube with internal diameters of 16 mm (1 mm thick), 18 mm (1 mm thick), and 20 mm (2.5 mm thick), were used. The PTFE material was chosen for its considerable charge density and extraordinary hydrophobicity, a combination that kept any left-over liquid from the experiments off the surface, averting any feasible disruption to succeeding signal calculations (Wang et al., 2020). Deionized water was utilized as the flow source to preserve signal integrity, thus minimizing the impact of impurities found in tap water. This choice ensures accurate measurements and reliable data throughout the experiment.

2.3 WF-TENGs friction electrode fabrication

The experiments involved two different friction electrode structures, requiring discrete steps for making the PTFE

friction electrodes. To initially explore whether the solid–liquid contact process in the circulating water tank could yield significant signals, we observed the signals generated using a TENG structured in the form of a blade. To make this blade structure, we employed 3D printing technology to produce the blade using the acrylonitrile butadiene styrene material. Then, a Cu film was applied to the surface of the blade, followed by a PTFE film, as depicted in Figure 2(a). The completed blade structure was mounted and securely fixed within the water tank. The rotation of the blade was driven by the flowing water, ensuring intermittent contact between PTFE and water. This arrangement enabled the measurement of signals produced by the friction generated when the flowing water comes into contact with the blade structure.

As the use of the first structure was unable to comprehensively explore the primary factors influencing the performance of WF-TENGs, we employed a different approach by attaching a Cu film to the outer surface of the PTFE tube, as depicted in Figure 2(b). The reason for adopting this configuration is to respond to certain limitations of the 3D-printed structure. Over time, the 3D-printed structure may develop gaps, which could lead to wetting of the Cu film after prolonged water immersion that, in turn, could

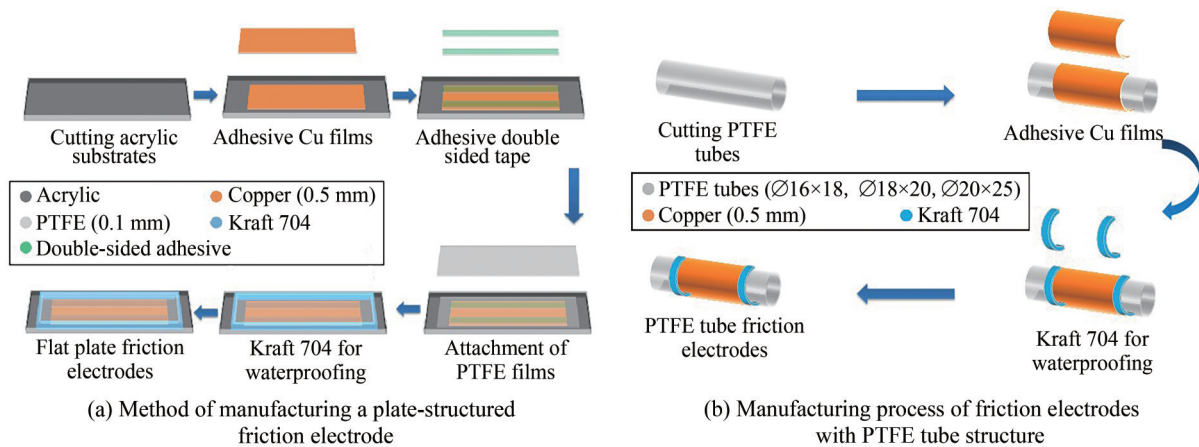


Figure 2 Fabrication process of the friction electrode

have a more significant impact on the ultimate signal generated. Moreover, the use of the TENG with the blade structure was unable to fully elucidate the main influencing factors, as the signal changes were not distinctly evident when altering the flow rate. By attaching the Cu film to the PTFE tube, we aimed to surpass these constraints and facilitate a more thorough investigation into the key factors affecting the performance of WF-TENGs. This experimental setup allowed for a more precise and detailed analysis of the generated signals and their correlation with the variations in flow rate, thus contributing to a deeper understanding of the overall system behavior.

3 Results and discussion

3.1 Principles of operation of WF-TENGs

WF-TENGs have a single-electrode configuration, where the friction electrode consists of a PTFE friction layer coupled with a Cu electrode. Electrical charge is generated through the solid–liquid contact friction when water passes over the friction electrode, facilitated by the interaction between PTFE and water. Then, this charge is exported from the Cu electrode through the principle of electrostatic induction, as depicted in Figure 3.

To elaborate on the solid–liquid contact process, we partitioned water into continuous segments, utilizing the movement of these segments to elucidate the generation of the alternating current (AC) signal. As illustrated in Figure 3(a(i.)), when a water segment carrying a positive charge is yet to enter the PTFE environment, charge interaction is absent, resulting in no signal generation. With the continuous movement of the water segment, when it comes into contact with the PTFE surface, the PTFE gains a negative charge, inducing a positive charge on the Cu electrode to establish electrostatic equilibrium, as depicted in Figure 3(a(ii.)). Upon complete contact between a water

segment and the PTFE surface, electron movement occurs between the Cu electrode and the ground. This movement leads to alternating positive and negative peaks, as depicted in Figure 3(a(iii., iv.)). As the water continues to flow forward, as depicted in Figure 3(a(v., vi.)), the amplitude of the signal progressively increases. When the water entirely covers the PTFE, the signal achieves its maximum amplitude. This stage yields a stable, continuous, and periodic signal output, as illustrated in Figure 3(a(vii.)). The overall signal variations throughout this process are presented in Figure 3(b).

3.2 Investigation of the solid–liquid contact process of vane-type WF-TENGs

To investigate the signal changes in the solid–liquid contact process within the recirculating flume, an experimental investigation is conducted using a vane structure, as depicted in Figure 4(a). The constructed structure was firmly mounted inside the tank, and the output power of the drive motor was regulated using a speed controller to alter the flow rate of the water in the tank.

The results obtained from the acquired voltage, current, and charge signals, shown in Figures 4(b)–(d), revealed that, as the water propelled the blade structure to rotate, intermittent contact occurred between the front and rear blades and the water, resulting in corresponding changes in the electrical signals. Remarkably, because of the prolonged immersion time of the structure in the water, WF-TENGs exhibited substantial signals even when both the front and rear blades were not directly in contact with the water. However, the signal rapidly increased and underwent a particularly noticeable change when the blades were again in contact with the water. This observed phenomenon remained consistent across multiple experiments, regardless of the changes in the flow rate. Consequently, we can reasonably assume that, within the circulating water tank, PTFE and water undergo charge movement during contact, leading to

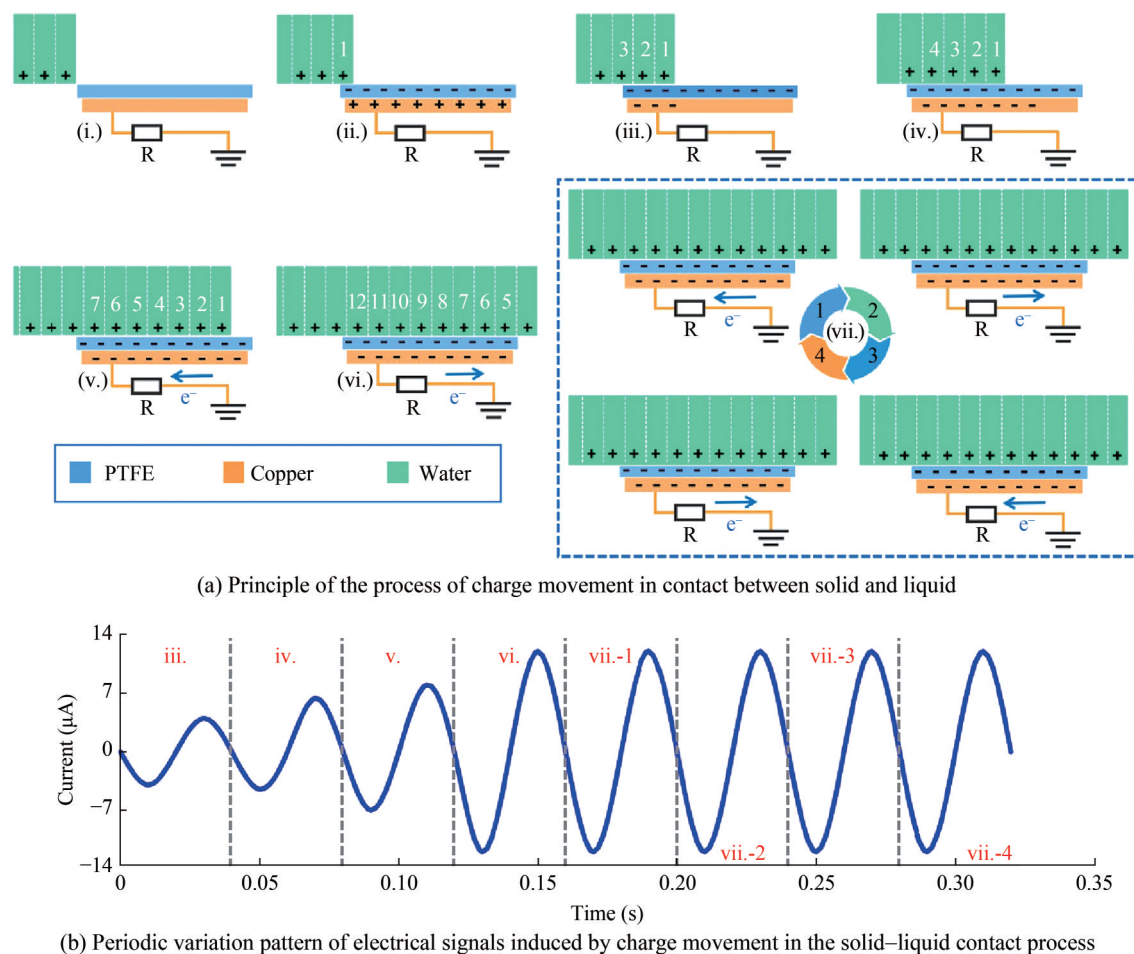


Figure 3 Charge generation process through solid-liquid contact

virtual displacement and, ultimately, generating evident electrical signals. Although this experiment successfully demonstrated a meaningful signal change during the contact and friction of water and PTFE, it did not exhibit significant variations when other conditions were altered. Therefore, further improvements and investigations are needed to enhance the performance of WF-TENGs under various conditions. The results shown in Figures 4(b)–(d) also indicate that, because of the intermittent contact between turbine blades and water during rotation, WF-TENGs cannot guarantee continuous and stable output. Therefore, to achieve stable output power, further exploration of other structural forms is needed.

3.3 Simulation of the solid-liquid contact process using COMSOL

The experiments conducted with blade structures demonstrated that the contact between PTFE and flowing water produces a significant signal. To gain a clearer and more intuitive understanding of the dynamic solid-liquid contact process and the distribution of electric potential,

finite element simulations were performed using the COMSOL Multiphysics software. The blade structure was simplified, and a flat plate was used instead to simulate the changes in electric potential during the solid-liquid contact process. A rectangular shape with gradually increasing length was employed to simulate the dynamic contact process between flowing water and PTFE. Finally, the distribution of electric potential was utilized to illustrate the phenomenon of contact between the two, resulting in the generation of electrical signals.

To simulate the changes in electric potential caused by the flowing water, a rectangular model with a height of 5 cm and a length increasing from 10 cm to 50 cm was constructed to represent the water droplet. A long rectangular strip measuring 50 cm in length and 1 cm in height was used to model the PTFE film. The distribution of electric potential for three typical states was calculated based on the length of the upper rectangular model. The dynamic process of water gradually covering the PTFE was simulated using a rectangular model with increasing length.

As shown in Figure 5, we note the changes in electric potential as the water droplet advances and engages with the PTFE surface. Initially, when the water first comes

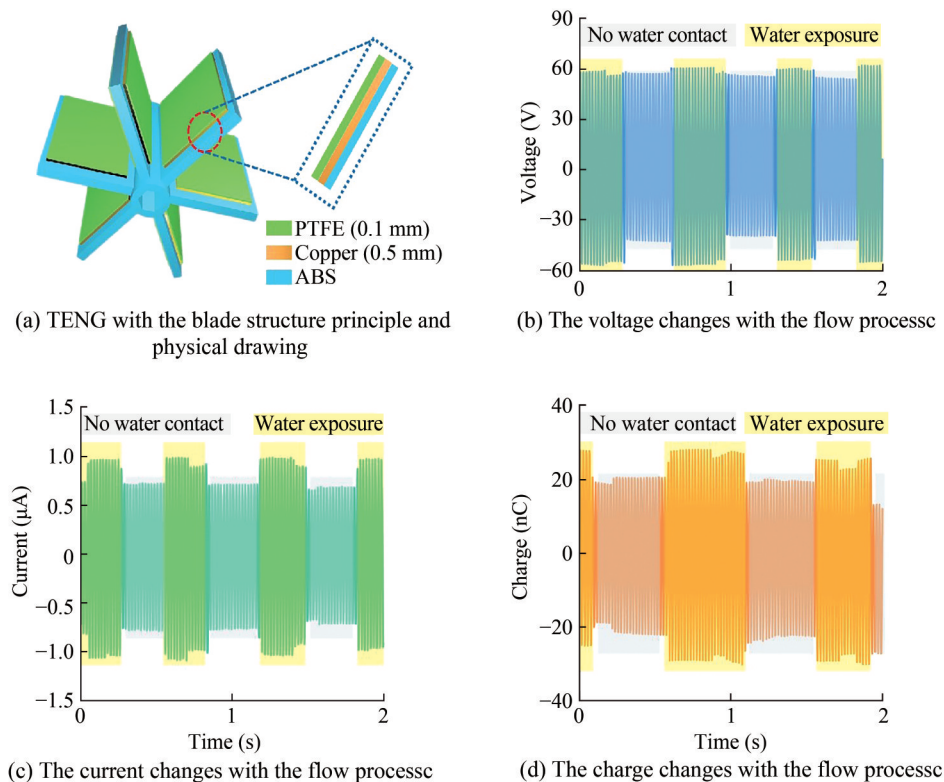


Figure 4 Results of signal variations of blade-type WF-TENGs

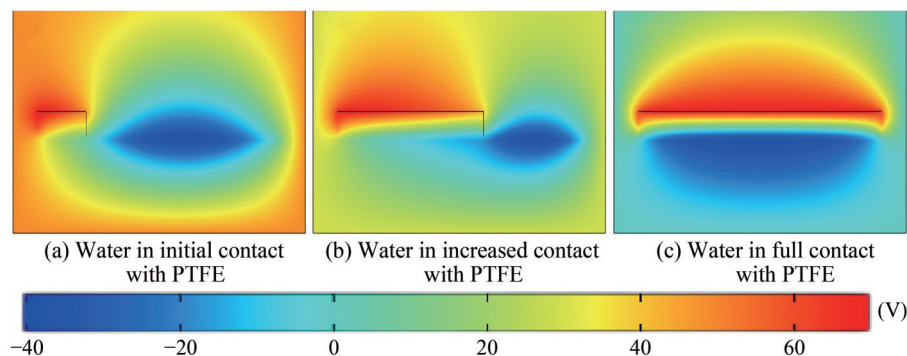


Figure 5 Potential change graph of the contact process between flowing water and PTFE

into contact with the PTFE, the destructive potential distribution is more pronounced. This phenomenon is attributed to the larger surface area of the PTFE than the water droplet, leading to an increased charge transfer and, consequently, a substantial potential difference. As the water droplet continues to flow forward, the positive potential on the graph becomes more blatant, whereas the angle between the zero potential surface and the PTFE surface decreases. Thus, a shift in the charge distribution is detected as the water moves along the PTFE surface. Furthermore, as the water droplet progresses and ensures complete contact with the PTFE, the contact area reaches its maximum. During this phase, the zero potential surface maintains a level position, whereas the surfaces of positive and negative potentials exhibit a symmetrical arrangement. This sym-

metrical distribution signifies a balanced charge transfer and potential difference. From Figure 6, we can observe and deduce that as the contact area between the water droplet and the PTFE surface increases, the resulting potential difference also slightly increases. This insight is critical to understanding the dynamics of the solid–liquid contact process in WF-TENGs and provides valuable information for optimizing their performance in capturing energy from flowing water.

3.4 Investigation of the factors affecting the performance of WF-TENGs

The initial blade structure test conducted in the circulating water tank, as described in Section 3.1, is successful in

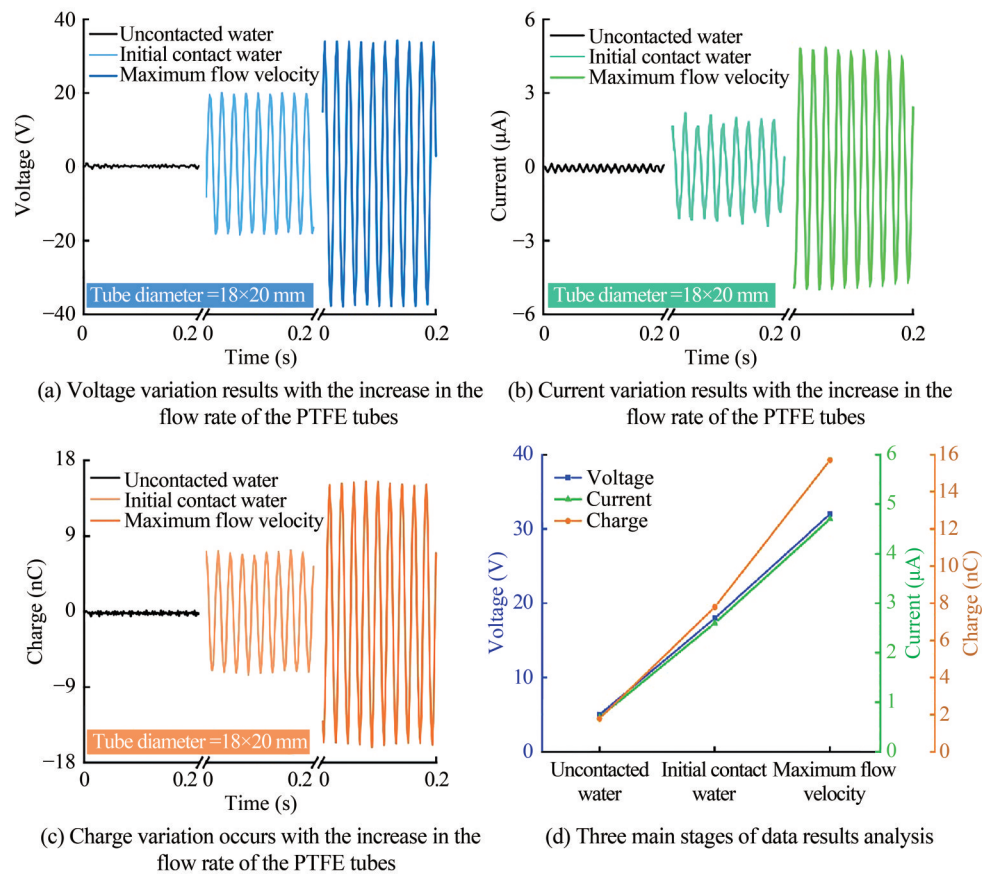


Figure 6 Detection results and analysis of TENG signals under different environmental parameters (18×20 mm)

demonstrating that flowing water can indeed make contact and friction with PTFE to generate noticeable electrical signals. Furthermore, simulation analysis has provided a comprehensive explanation of this phenomenon. Nevertheless, to gain a deeper insight into the factors affecting performance variations, additional detailed research is essential. In this regard, we have utilized PTFE tubes as the material for contact friction with flowing water. To construct the setup, we employed a laser cutting machine to precisely cut an appropriate acrylic plate, which enabled us to securely install the PTFE tubes in the tank while assuring that the Cu films were well sealed to prevent water from infiltrating it. This new experimental setup using the PTFE tubes will enable us to explore and analyze the intricate factors that affect the performance of WF-TENGs more comprehensively. By investigating the signal changes and potential distributions in this setup, we intend to obtain valuable insights that will aid in further improving the performance of WF-TENGs, specifically in capturing energy from flowing water and enhancing their overall efficiency.

To investigate the influence of flow rate on the output power of WF-TENGs, we conducted experiments using PTFE tubes with different diameters (i.e., 10×12, 12×14, 14×16, 16×18, 18×20, and 20×25 mm) and a length of

250 mm. On the surface of each tube, we attached a 20 cm long Cu film with the same thickness. Then, these structures were securely fixed within an acrylic holder, which was enclosed in the circulating water tank. To control the flow rate, we adjusted the output power of the drive motor using the speed controller. Once the flow rate stabilized, we recorded the electrical signals at three decisive moments: 1) when the water did not touch the PTFE tubes, 2) when the water just made contact with the tubes and filled their insides, and 3) when the maximum flow rate was achieved.

The output results show that, regardless of the diameter of the PTFE tube used, the output voltage, current, and charge signal all increase gradually with the increase in the flow velocity. Here, we present the output results for the 18×20 mm WF-TENGs, as shown in Figure 6. The results of WF-TENGs with other dimensions can be found in the Supplementary Materials. Figure 6(a) shows that the maximum voltage exceeds 30 V, Figure 6(b) indicates that the maximum current exceeds 4 μA , and similarly, Figure 6(c) shows that the maximum charge quantity exceeds 15 nC. By analyzing the optimal data for the three main parameters, as shown in Figure 6(d), we can intuitively observe from the figure that when water just makes contact with the PTFE, the flow velocity is at its minimum value. How-

ever, as the flow velocity quickly reaches its maximum, the signal output also increases rapidly. Therefore, within a certain velocity range, the increase in flow velocity will lead to an improvement in the output performance of WF-TENGs, which is of significance as a reference for collecting energy in high-velocity fluids.

By analyzing the information collected under the maximum flow velocity of PTFE tubes with different diameters, as shown in Figure 7(a), we determine that, except for the 20×25 mm tube, other PTFE tubes with the same thickness exhibit an increase in output signal with the increase in the diameter. However, further increasing the diameter to 20×25 mm leads to a rapid decrease in output. Considering this phenomenon, we change several variables. With the only change being an increase in thickness, we can conclude that the increase in thickness leads to a decrease in the average amplitude of the waveform. A larger thickness reduces the electrostatic force acting between the electrodes, resulting in a decrease in the induced charge quantity on the Cu electrode, ultimately leading to a sudden decrease in the collected signal.

The energy harvesting capability is an important performance indicator of TENGs. To further demonstrate the performance of WF-TENGs, we conducted charging experiments on different capacitors (i.e., 50 V–0.22 μF , 50 V–0.47 μF , and 50 V–1.0 μF) for the same duration (i.e., 240 s)

under maximum flow rate conditions. By comparing the charging voltages, the results shown in Figure 7(b) were obtained. The results indicate that, after the same duration, the charging voltages for the three different capacitors are 22, 14, and 8 V, indicating their good charging performance.

WF-TENGs can continuously output stable AC signals. To explore the variation of output power with load, the voltage and current were measured within the R_L range of 10 k Ω to 1 G Ω . The output shows that the voltage increases with the increase in the load resistance, whereas the current shows the opposite trend. The maximum power of WF-TENGs is not significant at 10 k Ω but reaches a maximum value of 7 μW at 10 M Ω , as shown in Figure 8(c). The long-term stability of WF-TENGs indicates that the signal output does not significantly decrease after 5 min, 1 week, 2 weeks, and 1 month, demonstrating that this method of collecting energy from flowing water exhibits good stability and durability.

During the experiment, an interesting observation regarding the signal generated when the water just touched the PTFE tube but did not fill it inside was made. Notably, in this scenario, the signal was relatively smaller than the signal observed when the tube was filled with water. Thus, we deduced that the contact area between the water and the PTFE surface could be a decisive factor influencing the signal output. To validate this assumption, we conducted

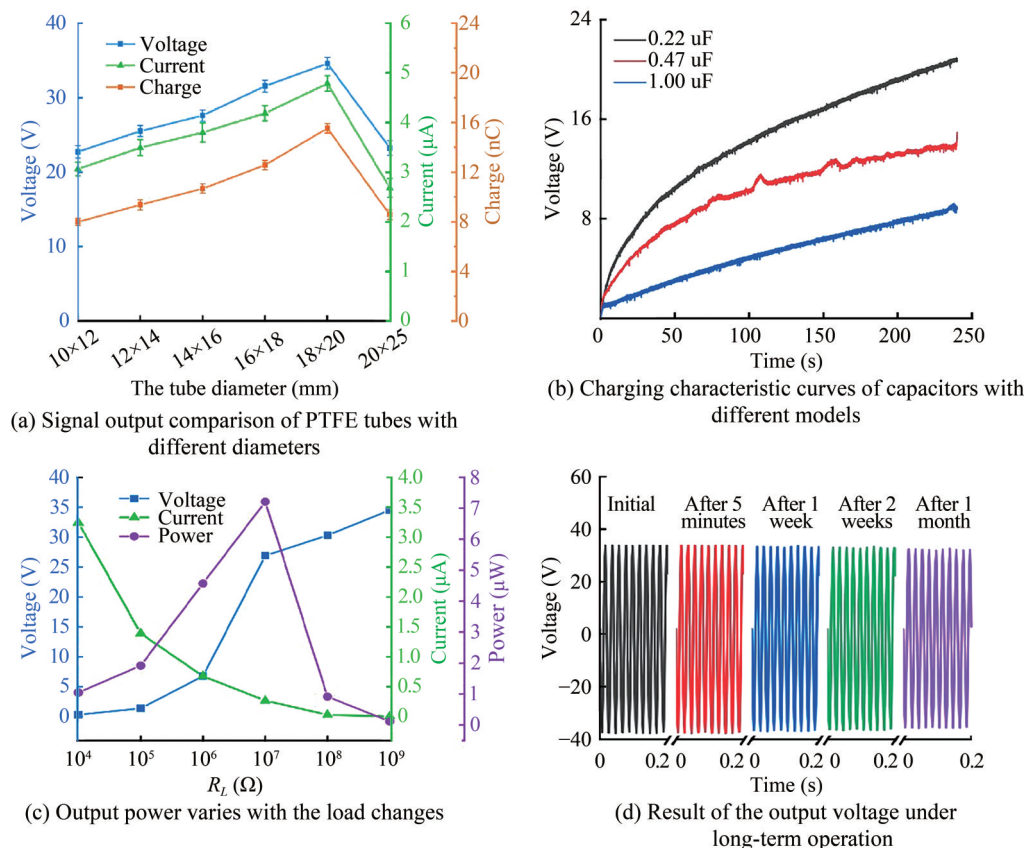


Figure 7 Key performance analysis of WF-TENGs

additional experiments by intersecting three PTFE tubes with a length of 250 mm and a diameter of 16×18 mm. Then, we attached Cu foils with varying lengths of 10, 15, and 20 cm to the top of these three tubes, as depicted in Figure 8(a), to control the size of the contact area between the water and the PTFE surface. After fixing the three tubes in the sink in the same manner as before, we measured the electrical signal output at the maximum flow rate. The experimental results, as shown in Figures 8(b)–(d), indicate that the output voltage, current, and charge signals gradually increase with the increase in the length of the Cu membrane, which is directly related to the increase in the contact area. This finding strongly supports our initial assumption, underscores the significance of the contact area in influencing the performance of WF-TENGs, and further highlights the importance of optimizing the contact area between the water and the PTFE surface to maximize the output power of the TENG. By carefully adjusting the size of the contact area, researchers can potentially improve the efficiency and overall performance of WF-TENGs in harvesting energy from flowing water.

3.5 Electrical energy harvesting for the WF-TENGs

Via a sequence of experiments and simulations conducted in the circulating water tank and by employing various friction electrode configurations, we have effectively pin-

pointed and examined the primary factors that influence the output power of the WF-TENGs. In particular, we determined that the thickness of the chosen friction material, the magnitude of the contact area between the water and the friction material, and the flow rate of the water are critical factors influencing the performance of solid–liquid TENGs. By meticulously managing and optimizing these influencing factors while ensuring that the chosen friction material remains unchanged, the output power and efficiency of the WF-TENGs can be substantially improved. These findings provide valuable insights and new ideas for future improvements in the design and performance of TENGs that harvest energy from flowing water. With the increasing need for sustainable and eco-friendly energy sources, the advancement of efficient energy-harvesting technologies becomes critically essential. The WF-TENGs, with their capability to harness the abundant energy present in flowing water, have great potential as a promising solution for clean and renewable energy generation. By understanding and addressing the key influencing factors revealed in this study, researchers can enhance the performance of WF-TENGs and unlock their full potential in realistic applications. In conclusion, the investigation into the principal factors affecting the output power of WF-TENGs represents a significant step forward in the development of water-energy-harvesting technologies, opens up new avenues for further research and progress in this field, and brings us closer to harnessing

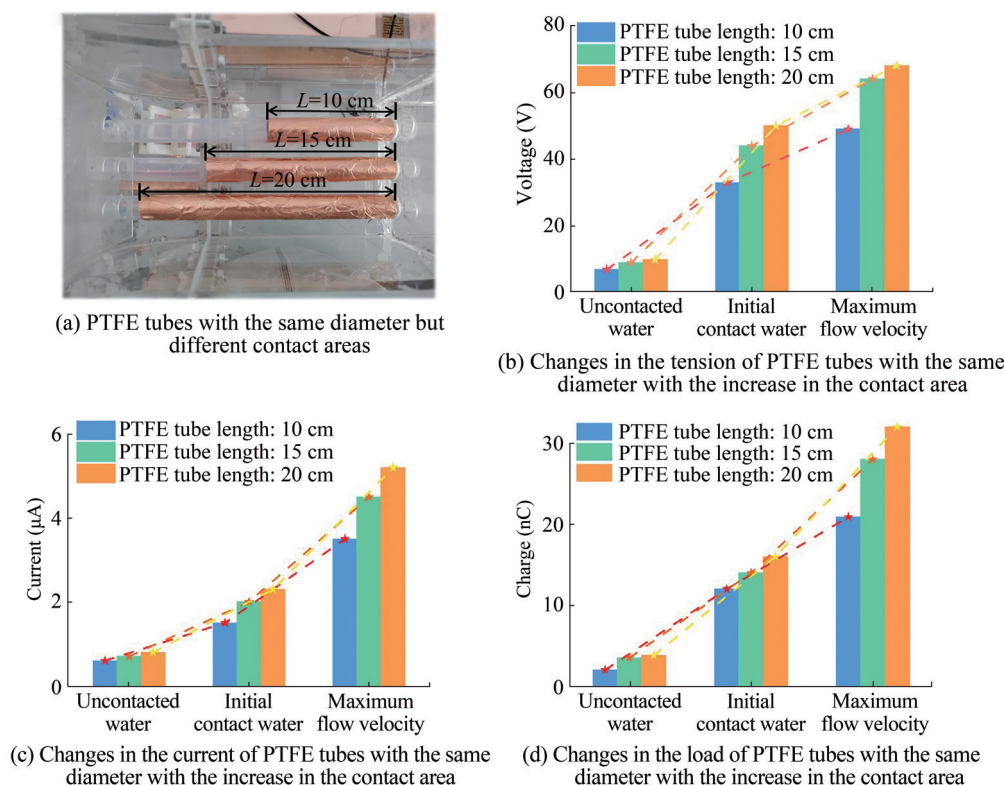


Figure 8 Impact of contact area on the signal results

the vast energy potential of flowing water as a sustainable and environmentally friendly energy source.

Optimizing the output performance of WF-TENGs is crucial for increasing power generation. In our study, we thoroughly investigated the main factors influencing the output performance to visualize the results by connecting a load. The circuit, as shown in Figure 9(a), was designed for the conversion and utilization of electrical energy. We used three PTFE tubes with a diameter of 18×20 mm and a length of 25 cm, with Cu films of 20 cm length affixed to each tube.

These tubes were arranged in parallel before being connected to the circuit. First, we opened switches S1, S2, and S4 and closed switch S3 to set the circuit in a self-testing state. We observed that the VL bulb was lit, indicating electrical output from the WF-TENGs. Then, we only closed switch S4 and connected the output of the circuit to an electrostatic meter to measure the output signal, obtaining voltage and current signals, as shown in Figures 9(b)

and (c). Notably, the output signal significantly increased compared with that of a single tube.

We conducted additional experiments with different combinations of switches to assess their impact on the output performance of WF-TENGs. When only switch S4 is closed, a row of LEDs connected to the output of P2 will light up immediately, but the brightness will be low. In another scenario, we first closed only switch S1, allowing capacitor C1 to charge for a while, and then closed switch S4. Interestingly, we observed that the brightness of the LEDs increased compared with the previous case, as shown in Figure 9(d). When initially only switch S2 is closed, allowing capacitor C2 to charge, and then switch S4 is closed, the LED brightness is higher than that of the two previous cases, as depicted in Figure 9(e). These experiments helped us understand how different switch configurations affect the output performance and provide valuable insights into enhancing the power generation efficiency of WF-TENGs.

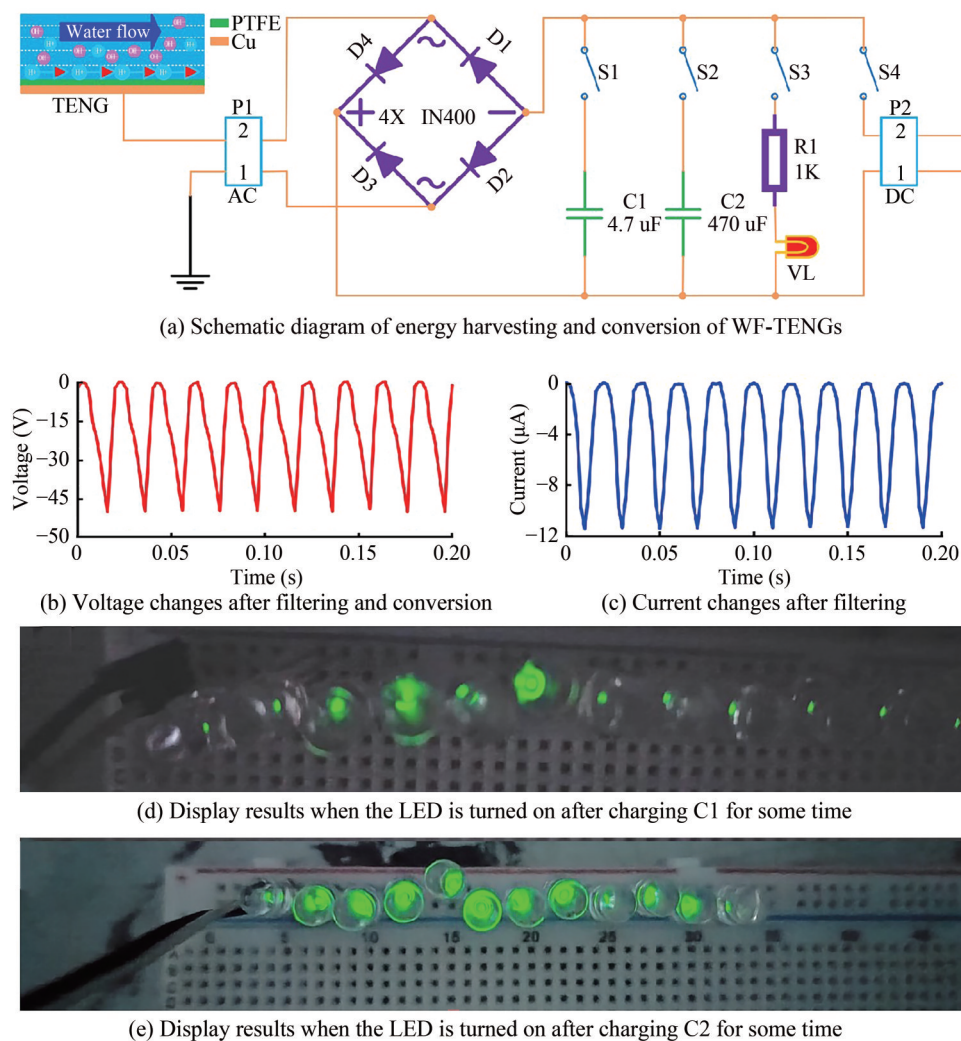


Figure 9 Process and results of energy harvesting and conversion

4 Conclusion

This study proposes a significant advancement in the field of water energy harvesting through the development of single-electrode-mode WF-TENGs and conducts experimental investigations in a circulating water tank. This research focuses on exploring the key factors influencing the output performance of solid–liquid TENGs operating in flowing water environments. Through methodical adjustments to the thickness and contact area of the friction material, coupled with the monitoring of the flow rate of the water, this study provides crucial insights into enhancing the power output of WF-TENGs. The experimental results indicate that the flow rate of the water plays a vital role in the power generation efficiency of WF-TENGs. With the increase in the flow rate, the output voltage, current, and charge signals noticeably increase, indicating a direct proportionality between the flow rate and the power output. Moreover, this study shows that the contact area between the solid friction material and the flowing water significantly affects the signal output. Larger contact areas lead to higher power generation, reinforcing the importance of efficient contact friction between the two surfaces. In addition, the thickness of the friction material is identified as another vital factor influencing the performance of WF-TENGs. Thicker friction materials result in greater potential differences and enhanced power output. This finding highlights the significance of selecting the appropriate materials and dimensions for friction electrodes in designing WF-TENGs. Furthermore, this study successfully converts and utilizes the collected electrical energy to power small electrical appliances through a filter circuit. This application demonstrates the practical potential of WF-TENGs in providing sustainable and efficient green energy.

In conclusion, this research contributes valuable knowledge to the development of WF-TENG technology for energy harvesting from flowing water. The investigated factors and experimental findings provide crucial guidance for optimizing the design and performance of WF-TENGs. This study paves the way for future advancements in water-energy-harvesting technology, opening up new possibilities for renewable energy sources and maintainable applications in various fields.

Acknowledgement The authors would like to acknowledge the support from Natural Science Foundation of Heilongjiang Province (No.YQ2022A004) and National Natural Science Foundation of China (No.12372268, No.12332014).

Competing interest Chengwang Xiong is an editorial board member for the Journal of Marine Science and Application and was not involved in the editorial review, or the decision to publish this article. All authors declare that there are no other competing interests.

References

- Armiento S, Filippeschi C, Meder F, Mazzolai B (2022) Liquid-solid contact electrification when water droplets hit living plant leaves. *Commun Mater* 3: 1-12. <https://doi.org/10.1038/s43246-022-00302-x>
- Baytekin HT, Patashinski AZ, Branicki M, Soh S, Grzybowski BA (2011) The mosaic of surface charge in contact electrification. *Science* 333: 308-312. <https://doi.org/10.1126/science.1201512>
- Cheng G, Zhang T, Fu X, Hua J, Dai W, Cao J, Sun W, Ding J (2024) A comprehensive review of advancements and challenges from solid–solid to liquid–solid triboelectric nanogenerators. *Advanced Materials Technologies* 9: 2301588. <https://doi.org/10.1002/admt.202301588>
- Choi D, Lee S, Park SM, Cho H, Hwang W, Kim DS (2015) Energy harvesting model of moving water inside a tubular system and its application of a stick-type compact triboelectric nanogenerator. *Nano Res* 8: 2481-2491. <https://doi.org/10.1007/s12274-015-0756-4>
- Chung J, Heo D, Kim B, Lee S (2018) Superhydrophobic water-solid contact triboelectric generator by simple spray-on fabrication method. *Micromachines* 9: 593. <https://doi.org/10.3390/mi9110593>
- Cui X, Yu C, Wang Z, Wan D, Zhang H (2022) Triboelectric nanogenerators for harvesting diverse water kinetic energy. *Micromachines* 13: 1219. <https://doi.org/10.3390/mi13081219>
- Fan FR, Lin L, Zhu G, Wu W, Zhang R, Wang Z (2012) Transparent triboelectric nanogenerators and self-powered pressure sensors based on micropatterned plastic films. *Nano Lett* 12: 3109-3114. <https://doi.org/10.1021/nl300988z>
- Feng T, Ling D, Li C, Zheng W, Zhang SLi C, Yanov AE, Pozdnyakov AS, Lu L, Mao Y (2024) Stretchable on-skin touchless screen sensor enabled by ionic hydrogel. *Nano Res* 17: 4462-4470. <https://doi.org/10.1007/s12274-023-6365-8>
- Gao H, Hu M, Ding J, Xia B, Yuan G, Sun H, Xu Q, Zhao S, Jiang Y, Wu H, Yuan M, Li J, Li B, Zhao J, Rao D, Xie Y (2023) Investigation of contact electrification between 2D MXenes and MoS₂ through density functional theory and triboelectric probes. *Advanced Functional Materials* 33: 2213410. <https://doi.org/10.1002/adfm.202213410>
- Hu S, Shi Z, Zheng R, Ye W, Gao X, Zhao W, Yang G (2020) Superhydrophobic liquid–solid contact triboelectric nanogenerator as a droplet sensor for biomedical applications. *ACS Appl Mater Interfaces* 12: 40021-40030. <https://doi.org/10.1021/acsami.0c10097>
- Jiang L, Lu G, Zeng Y, Sun Y, Kang H, Burford J, Gong C, Humayun M S, Chen Y, Zhou Q (2022) Flexible ultrasound-induced retinal stimulating piezo-arrays for biomimetic visual prostheses. *Nat Commun* 13: 3853. <https://doi.org/10.1038/s41467-022-31599-4>
- Lee JH, Kim S, Kim TY, Khan U, Kim S W (2019) Water droplet-driven triboelectric nanogenerator with superhydrophobic surfaces. *Nano Energy* 58: 579-584. <https://doi.org/10.1016/j.nanoen.2019.01.078>
- Li J, Carlos C, Zhou H, Sui J, Wang Y, Silva-Pedraza Z, Yang F, Dong Y, Zhang Z, Hacker T A, Liu B, Mao Y, Wang X (2023a) Stretchable piezoelectric biocrystal thin films. *Nat Commun* 14: 6562. <https://doi.org/10.1038/s41467-023-42184-8>
- Li J, Long Y, Yang F, Wang X (2020) Respiration-driven triboelectric nanogenerators for biomedical applications. *EcoMat* 2: e12045. <https://doi.org/10.1002/eom2.12045>
- Li X, Tao J, Wang X, et al (2018) Networks of high performance triboelectric nanogenerators based on liquid–solid interface contact electrification for harvesting low-frequency blue energy. *Advanced Energy Materials* 8: 1800705. <https://doi.org/10.1002/>

- aenm.201800705
- Li X, Zhang D, Zhang D, Zhu J, Pan C, Wang Z L (2023b) Solid-liquid triboelectric nanogenerator based on vortex-induced resonance. *Nanomaterials* 13: 1036. <https://doi.org/10.3390/nano13061036>
- Li X, Zhou Y, Li Z, Guo H Y, Gong Y, Zhang D, Zhang Q, Zhang B, Wang B, Peng Y (2023c) Vortex-induced vibration triboelectric nanogenerator for energy harvesting from low-frequency water flow. *Energy Conversion and Management* 292: 117383. <https://doi.org/10.1016/j.enconman.2023.117383>
- Li Z, Wang C, Gong Y, Zhou Y, Zhang D, Peng Y, Wu H (2024) The investigation of V-shaped arrays with non-uniform diameter cylinders for high performance hydrokinetic energy conversion. *Ocean Engineering* 295: 116689. <https://doi.org/10.1016/j.oceaneng.2024.116689>
- Li Z, Yang D, Zhang Z, Lin SQ, Cao B, Wang LM, Wang ZL, Yin FH (2022) A droplet-based electricity generator for large-scale raindrop energy harvesting. *Nano Energy* 100: 107443. <https://doi.org/10.1016/j.nanoen.2022.107443>
- Lin H, He M, Jing Q, Yang W, Wang S, Liu Y, Zhang Y, Li J, Li N, Ma Y, Wang L, Xie Y (2019) Angle-shaped triboelectric nanogenerator for harvesting environmental wind energy. *Nano Energy* 56: 269-276. <https://doi.org/10.1016/j.nanoen.2018.11.037>
- Lin S, Xu C, Xu L, Wang ZL (2020) The overlapped electron-cloud model for electron transfer in contact electrification. *Advanced Functional Materials* 30: 1909724. <https://doi.org/10.1002/adfm.201909724>
- Liu Y, Sun N, Liu J, Wen Z, Sun X, Lee S T, Sun B (2018) Integrating a silicon solar cell with a triboelectric nanogenerator via a mutual electrode for harvesting energy from sunlight and raindrops. *ACS Nano* 12: 2893-2899. <https://doi.org/10.1021/acsnano.8b00416>
- McCarty LS, Whitesides GM (2008) Electrostatic charging due to separation of ions at interfaces: Contact electrification of ionic electrets. *Angewandte Chemie International Edition* 47: 2188-2207. <https://doi.org/10.1002/anie.200701812>
- Mondal R, Hasan MAM, Zhang R, Olin H, Yang Y (2022) Nanogenerators-based self-powered sensors. *Advanced Materials Technologies* 7: 2200282. <https://doi.org/10.1002/admt.202200282>
- Mudgal T, Tiwari M, Bharti D (2024) Cylindrical-electrode triboelectric nanogenerator for low-speed wind energy harvesting. *Nano Energy* 123: 109388. <https://doi.org/10.1016/j.nanoen.2024.109388>
- Munirathinam K, Kim DS, Shanmugasundaram A, Park J, Jeong Y J, Lee D W (2022) Flowing water-based tubular triboelectric nanogenerators for sustainable green energy harvesting. *Nano Energy* 102: 107675. <https://doi.org/10.1016/j.nanoen.2022.107675>
- Nguyen QT, Ahn KK (2021) Fluid-based triboelectric nanogenerators: A review of current status and applications. *Int J of Precis Eng and Manuf-Green Tech* 8: 1043-1060. <https://doi.org/10.1007/s40684-020-00255-x>
- Nguyen QT, Vu DL, Le CD, Ahn KK (2023a) Enhancing the performance of triboelectric generator: A novel approach using solid-liquid interface-treated Foam and metal contacts. *Polymers* 15: 2392. <https://doi.org/10.3390/polym15102392>
- Nguyen QT, Vu DL, Le CD, Ahn KK (2023b) Recent progress in self-powered sensors based on liquid-solid triboelectric nanogenerators. *Sensors* 23: 5888. <https://doi.org/10.3390/s23135888>
- Nie J, Wang Z, Ren Z, Li S, Chen X, Wang Z L (2019) Power generation from the interaction of a liquid droplet and a liquid membrane. *Nat Commun* 10: 2264. <https://doi.org/10.1038/s41467-019-10232-x>
- Niu J, Xu W, Tian K, He G, Huang Z, Wang Q (2020) Triboelectric energy harvesting of the superhydrophobic coating from dropping water. *Polymers* 12: 1936. <https://doi.org/10.3390/polym12091936>
- Rayegani A, Saberian M, Delshad Z, Liang J, Sadiq M, Nazar AM, Mohsan SAH, Khan MA (2023) Recent advances in self-powered wearable sensors based on piezoelectric and triboelectric nanogenerators. *Biosensors* 13: 37. <https://doi.org/10.3390/bios13010037>
- Sun M, Lu Q, Wang ZL, Huang B (2021) Understanding contact electrification at liquid-solid interfaces from surface electronic structure. *Nat Commun* 12: 1752. <https://doi.org/10.1038/s41467-021-22005-6>
- Tan D, Zeng Q, Wang X, Yuan S, Luo Y, Zhang X, Tan L, Hu C, Liu G (2022) Anti-overtuning fully symmetrical triboelectric nanogenerator based on an elliptic cylindrical structure for all-weather blue energy harvesting. *Nano-Micro Lett* 14: 124. <https://doi.org/10.1007/s40820-022-00866-w>
- Vu DL, Nguyen QT, Chung PS, Ahn KK (2024) Self-powered flow rate sensing via a single-electrode flowing liquid based triboelectric nanogenerator. *Micromachines* 15: 384. <https://doi.org/10.3390/mi15030384>
- Wang H, Xu L, Wang Z (2021) Advances of high-performance triboelectric nanogenerators for blue energy harvesting. *Nanoenergy Advances* 1: 32-57. <https://doi.org/10.3390/nanoenergyadv1010003>
- Wang J, Chen X, Sun Y, Qin X (2024) A natural-light-enabled self-powered system simultaneously monitoring wind speed, humidity, and irradiance in multiple channels. *Nano Energy* 123: 109364. <https://doi.org/10.1016/j.nanoen.2024.109364>
- Wang J, Wu C, Dai Y, Zhao Z, Wang A, Zhang T, Wang Z L (2017) Achieving ultrahigh triboelectric charge density for efficient energy harvesting. *Nat Commun* 8: 88. <https://doi.org/10.1038/s41467-017-00131-4>
- Wang N, Liu Y, Ye E, Wang D (2023a) Innovative technology for self-powered sensors: Triboelectric nanogenerators. *Advanced Sensor Research* 2: 2200058. <https://doi.org/10.1002/adsr.202200058>
- Wang N, Liu Y, Ye E, Li Z, Wang D (2023b) Contact electrification behaviors of solid-liquid interface: Regulation, mechanisms, and applications. *Advanced Energy and Sustainability Research* 4: 2200186. <https://doi.org/10.1002/aesr.202200186>
- Wang S, Lin L, Xie Y, Jing Q, Niu S, Wang ZL (2013) Sliding-triboelectric nanogenerators based on in-plane charge-separation mechanism. *Nano Lett* 13: 2226-2233. <https://doi.org/10.1021/nl400738p>
- Wang S, Xu J, Wang W (2018) Skin electronics from scalable fabrication of an intrinsically stretchable transistor array. *Nature* 555: 83-88. <https://doi.org/10.1038/nature25494>
- Wang Y, Gao S, Xu W, Wang Z (2020) Nanogenerators with superwetting surfaces for harvesting water/liquid energy. *Advanced Functional Materials* 30: 1908252. <https://doi.org/10.1002/adfm.201908252>
- Wang ZL (2013) Triboelectric nanogenerators as new energy technology for self-powered systems and as active mechanical and chemical sensors. *ACS Nano* 7: 9533-9557. <https://doi.org/10.1021/nn404614z>
- Wang ZL (2020) On the first principle theory of nanogenerators from Maxwell's equations. *Nano Energy* 68: 104272. <https://doi.org/10.1016/j.nanoen.2019.104272>
- Wu M, Zhu C, Si J, Wang H, Xu M, Mi J (2023) Recent progress in flow energy harvesting and sensing based on triboelectric nanogenerators. *Advanced Materials Technologies* 8: 2300919. <https://doi.org/10.1002/admt.202300919>

- Xu M, Wang S, Zhang SL, Kien PT, Chuan W, Li ZH, Wang ZL (2019) Highly-sensitivity and self-powered ocean wave sensor based on liquid-solid interfacing triboelectric nanogenerator. *Meet Abstr MA2019-02*: 2255. <https://doi.org/10.1149/MA2019-02/51/2255>
- Xue E, Guo Z, Zhao H, Yuan C (2022) A review of the design and feasibility of intelligent water-lubrication bearings. *J Marine Sci Appl* 21: 23-45. <https://doi.org/10.1007/s11804-022-00296-5>
- Ye C, Liu D, Chen P, Cao L, Li XJ, Jiang T, Wang Z L (2023) An integrated solar panel with a triboelectric nanogenerator array for synergistic harvesting of raindrop and solar energy. *Advanced Materials* 35: 2209713. <https://doi.org/10.1002/adma.202209713>
- Zhang C, Yang X, Zhang B, Fan KQ, Liu ZM, Liu Z (2023) The efficient energy collection of an autoregulatory driving arm harvester in a breeze environment. *Micromachines* 14: 2032. <https://doi.org/10.3390/mi14112032>
- Zhang X, Yu M, Ma Z, Ouyang H, Zou Y, Zhang SL, Niu H, Pan X, Xu MY, Li Z, Wang Z L (2019) Self-powered distributed water level sensors based on liquid–solid triboelectric nanogenerators for ship draft detecting. *Advanced Functional Materials* 29: 1900327. <https://doi.org/10.1002/adfm.201900327>
- Zhao XJ, Wang HL, Wang ZL, Wang J (2024) Nanocomposite electret layer improved long-term stable solid–liquid contact triboelectric nanogenerator for water wave energy harvesting. *Small* 20: 2310023. <https://doi.org/10.1002/sml.202310023>
- Zou Y, Gai Y, Tan P, Jiang D, Qu X, Xue J, Ouyang H, Shi BJ, Li LL, Luo D, Deng YL, Li Z, Wang Z L (2022) Stretchable graded multichannel self-powered respiratory sensor inspired by shark gill. *Fundamental Research* 2: 619-628. <https://doi.org/10.1016/j.fmre.2022.01.003>